

Small biochar particles hardly disintegrate under cryo-stress

Gabriel Sigmund^{a,*}, Andrea Schmid^a, Hans-Peter Schmidt^b, Nikolas Hagemann^{b,c},
Thomas D. Bucheli^c, Thilo Hofmann^a

^a Environmental Geosciences, Centre for Microbiology and Environmental Systems Science, University of Vienna, Vienna 1090, Austria

^b Ithaka Institute, Ancienne Eglise 9, 1974 Arbaz, Switzerland

^c Environmental Analytics, Agroscope, 8046 Zürich, Switzerland

ARTICLE INFO

Handling Editor: Matthew Tighe

Keywords:
Biochar
Disintegration
Freeze–thaw
Carbon

ABSTRACT

Physical disintegration of biochar has been postulated to determine the persistence and mobility in soil of this recalcitrant carbon pool. Therein, freeze–thaw cycling can induce substantial physical stress to biochars. We here investigated the physical disintegration and subsequent mobilisation of five different biochars under “realistic worst-case scenarios” in a laboratory soil column setup as well as in shaking and sonication batch experiments. The mobilization of carbon from biochar particles (0.25–1 mm) was investigated in the absence of clay at a pH of 6.3 with and without 80 freeze–thaw cycles. The small biochar particles used in this study did not strongly disintegrate after freeze–thaw cycling, possibly because of freezing point depression in biochar micropores. Our results in comparison with findings in literature suggest that freeze–thaw-induced physical disintegration of biochar is a process more pronounced for large biochar particles containing substantial *meso*- and *macro*pores. Biochars with larger ash fractions disintegrated more, presumably because of the ash-associated formation of unstable cavities within the biochar. Physical stability of biochars produced from the same feedstock at different pyrolysis temperatures decreased with increasing aromaticity, which may be linked to a higher rigidity of more aromatic structures. Moisture content in the soil increased carbon mobilization from biochar more than physical stress such as freeze–thaw cycling. The physical disintegration of biochar and subsequent mobilization of micro- and nanosized carbon should thus be considered of minor relevance and is often not a driving factor for biochar stability in soil.

1. Introduction

Physical disintegration of biochar was suggested to be a major process determining biochar mobility and stability in soil, with implications for biochar use in e.g. agriculture, carbon sequestration as well as soil remediation. Spokas et al., (2014) investigated the disintegration of 10 biochars and measured mass loss of ~6 to 35 % in batch-shaking experiments. This suggests that biochar disintegration may diminish long-term biochar carbon sequestration in soil because increasing surface area to volume ratios with decreasing particle size are expected to cause more reactive particles, which may thus degrade more readily. In addition, smaller particles may be transported through the soil pore structure more easily. When biochar is applied to very sandy soils, a considerable carbon fraction could thus be mobilized and potentially degraded. In contrast, in soils with average clay contents, small biochar particles would quickly interact with clay particles acting as binding

agents to form stable biochar-clay aggregates which are not easily mobilized or degraded (Schiedung et al., 2020; Yang et al., 2022; Bowring et al., 2022).

Most studies on biochar disintegration were conducted under conditions hardly relatable to field settings. A number of authors used shaking or sonication-based batch experiments to disintegrate biochar into micro- and nanoparticles and investigate some of their behaviors (Qu et al., 2016; Song et al., 2019; Xing et al., 2018). These studies found that biochar produced at low temperatures (≤ 350 °C) with a relatively low degree of carbonization and a correspondingly high aliphatic fraction was more prone to physically disintegrate, in part because of the higher solubility of the aliphatic fractions compared to the more aromatic fractions in biochar produced at higher temperatures (≥ 400 °C) (Keiluweit et al., 2010; Santin et al., 2017). Accordingly, Song et al. (2019) found that the particulate organic carbon fraction that can be mobilized is more polar and less aromatic than the bulk material it is

* Corresponding author.

E-mail address: gabriel.sigmund@univie.ac.at (G. Sigmund).

<https://doi.org/10.1016/j.geoderma.2023.116326>

Received 21 June 2022; Received in revised form 2 January 2023; Accepted 3 January 2023

Available online 6 January 2023

0016-7061/© 2023 The Author(s). Published by Elsevier B.V. This is an open access article under the CC BY license (<http://creativecommons.org/licenses/by/4.0/>).

released from.

Most prior studies relating to physical disintegration and the leaching of organic matter from biochar analysed the “dissolved” organic carbon content (DOC) using operational cut offs such as $<0.45 \mu\text{m}$ (Liu et al., 2018; Qu et al., 2016). However, the quantification of the mobilized total organic carbon (TOC) capable to pass through soil may be more meaningful for mass balance purposes, as this fraction also includes mobilized micro- and nanoparticles. To date, it remains unclear, how findings from batch studies can be translated to soil systems, where the physical stress on biochar particles is substantially smaller, and the liquid-to-solid ratio is orders of magnitude lower. Liu et al., (2018) are among the few authors that investigated biochar particle disintegration under soil-like conditions, by applying freeze–thaw cycles to one biochar. Focusing on macroscopic changes in the biochar particles, the authors found that bulk biochar particles became smaller after freezing and the $\text{Diameter}_{\text{min}}/\text{Diameter}_{\text{max}}$ ratio changed (Liu et al., 2018).

Under varying environmental conditions, the physical disintegration of biochar could additionally be affected by the biochar’s porosity and water-holding capacity (WHC), which is known to increase with increasing pyrolysis temperature (Brewer et al., 2014; Edeh et al., 2020). Biochar porosity and physical structure is also highly affected by the type of feedstock: grassy feedstocks result in biochars with high macroporosity which is easily capable to uptake water compared to more microporous biochar from woody feedstocks (Brewer et al., 2014). Freeze–thaw cycling may thus substantially contribute to the physical disintegration of biochar and could have underexplored consequences for biochar stability in the field. The physical disintegration of biochar under cryo-stress and subsequent mobilization of micro- and nanosized carbon should thus be investigated to assess its relevance for biochar stability compared to chemical oxidation and biological degradation of the bulk biochar.

Here, we investigate the disintegration of small biochar particles (0.25–1 mm) in sand columns exposed to freeze–thaw cycles under different water saturation conditions and compare findings with parallel batch experiments. To cover a range of scenarios, we studied five different biochars intermixed at 5 % wt into pure sand columns. The aim was to investigate a high mobilization scenario with no clay present, and a relatively high pH (6.3) to maximize DOM dissolution and particle mobilization due to increased electrostatic repulsion from negatively charged surface groups. The experiments were conducted at two different moisture conditions (at 50 % and 120 % water holding capacity) using standardized artificial rainwater with a relatively low ionic strength to obtain a realistic “worst case” scenario in relation to carbon mobilization. In the field, the largest carbon losses from biochar are observed within the first year after field application due to the leaching and degradation of labile biochar fractions during that time (Wang et al., 2016). Accordingly, we investigated the physical disintegration of biochar for freeze–thaw cycles corresponding to approximately one year of field ageing in temperate climatic regions (80 cycles).

2. Material and methods

2.1. Materials and chemicals

Standardized biochar produced from softwood pellets (SWP) and Miscanthus pellets (MSP) at pyrolysis temperatures of 500 or 700 °C, were purchased from the UK Biochar research centre and will be referred to as SWP500, SWP700, MSP500, and MSP700. In addition, wine pruning biomass was pyrolyzed in a traditional Kon-Tiki approach followed by wet quenching with water, which will be referred to as “vine Kon Tiki”. Large biochar particles were gently crushed and sieved, using the biochar particle size fraction 0.25–1 mm for all experiments. Dorsilit® quartz sand (0.3–0.8 mm grain size) was muffled at 550 °C for 5 h prior to use. Artificial rainwater at pH 6.3 was produced following a protocol by Ricci et al., (2010) using analytical grade chemicals purchased from Merck and Sigma Aldrich (see [Supporting Information](#) for

details). All glassware used for experimentation was muffled at 550 °C for 5 h prior to use.

2.2. Biochar characterization

The CHNS composition of biochar was determined according to DIN 51732 via TruSpec CHN (Leco), ash content was determined from dry materials burned at 750 °C for 6 h. Oxygen content was determined via mass balance assuming that $\% \text{O} = 100 - \sum \% (\text{C, H, N, S, ash})$. Total pore volume and pore size distributions were determined via N_2 physisorption as previously described in Sigmund et al. (2017). Bulk properties of the standard materials from the UK Biochar research centre were compared to the producer’s measurements. Minor differences observed are likely related to batch to batch variation as well as a possible size fractionation during sieving.

2.3. Freeze–thaw column experiments

To test a large number of scenarios we developed a small-scale column setup that can easily be transported and frozen. In short, we built holding racks to move and handle groups of columns built out of 50 mL syringes purchased from VWR. A small layer (approximately 5 mm) of previously muffled glass wool was placed at the bottom of the syringe to prevent sand from trickling out of the column. The column was subsequently filled up with 30 g sand–biochar mixtures (or sand without biochar as a control). The rack was then placed into a box filled with artificial rainwater for 24 h. Following this incubation, we used gravity drainage and weighed the drained column to calculate the respective water holding capacity (WHC). Subsequently each column was rinsed with 240 mL of rainwater to wash out those biochar fractions that would have been mobile prior to the freeze–thaw experiment (corresponds to approx. 25 pore volumes). This “rinsing” fraction was collected and characterized for pH, electrical conductivity, TOC (Shimadzu TOC-L analyzer), the particles size distribution (EyetechnTM from Ambivalue), and Zeta Potential (Malvern ZetaSizer Nano) as well as the DOC ($<0.45 \mu\text{m}$ fraction) and the DOC absorbance at 254 nm (Perkin Elmer, Lambda 35 UV–vis Spectrophotometer) to calculate the aromaticity proxy SUVA_{254} (Weishaar et al., 2003). More analytical details can be found in the [supporting information](#).

For the main experiment, the water volume in the columns was adjusted to either (i) 50 % of WHC by drying the saturated columns in an oven at 40 °C until the desired weight of the columns was reached or (ii) 120 % of WHC by adding artificial rainwater to the columns using a pipette. Subsequently, the syringe was sealed using a Luer lock at the tip and covered with Parafilm at the top. To emulate freeze–thaw cycles, the sealed syringes were frozen for 8 h at $-20 \text{ }^\circ\text{C}$ and thawed at room temperature (25 °C) for approximately 16 h before being frozen again. This approach was used to simulate 80 freeze–thaw cycles for all six biochars at both moisture conditions, respectively. The selected 80 freeze–thaw cycles are at the upper annual limit of temperate climate zones (Freeze–Thaw Days, 2022). At the end to the freeze–thaw cycles, the columns were rinsed with 50 mL of artificial rainwater (approx. 5 pore volumes) to subsequently measure the beforementioned parameters. To approximate the annual precipitation in temperate climates, for total carbon measurements, another 400 mL of artificial rainwater were used for rinsing and subsequent carbon analysis with the 80-freeze–thaw cycle scenario (corresponding to a total of 750 mm precipitation relative to the column surface). In addition, for all Biochar–sand combinations, and both WHCs, columns were stored at 25 °C without the freeze–thaw cycling as a control group for the duration of the experiment to account for slow dissolution processes. The artificial rainwater additionally contained 20 mg/L NaN_3 to suppress microbial activity in the columns. All carbon analyses were blank-corrected for measurements from sand columns without biochar addition. The glass wool layer as used here had a size cutoff of approximately 10 μm . Based on pre-experiments, this cutoff did not influence our results, as the overwhelming majority of

particles (>99 %) was smaller than 10 μm . Large biochar particles remaining in the columns were characterized for CHNS composition at the end of the experiments to investigate changes in the bulk composition. An exact quantification of oxygen for these samples was not possible due to limited sample amount recovered from the columns for measuring ash content.

2.4. Shaking and sonication batch experiments

To make batch experiments comparable to the abovementioned column setup, the gravity drainage step described above was done for all biochars prior to batch experimentation. After this rinsing step, the biochar was dried at 40 °C for 48 h and thereafter used for batch experiments. Two different batch setups were used and compared for all biochar samples. Firstly, the shaking protocol from Spokas et al., (2014) was adapted using the same solid to liquid ratio (1:20) and shaking biochar suspension for 24 h at 125 rpm in the dark. Secondly, identical biochar suspensions were not shaken but sonicated in glass vials for 10 min using a Bandelin sonorex super rk106 bath (35 kHz). Following the batch disintegration experiments, the suspensions were run through an empty column with glass wool to increase comparability with the column setup. The resulting suspensions were analyzed via the same procedures as described in 2.3. Additionally, the residual solid particles were recovered from the glass wool in the syringe and used for CHNS analysis.

2.5. Data analysis

Experiments were done in triplicates for subsequent statistical analysis which was performed using Origin Pro 2018b. Groups of scenarios investigated were compared using two-sided ANOVA. Figures were plotted with error bars which represent calculated standard deviations.

3. Results and discussion

In the subsequent sections it should be noted that a small cumulative fraction of carbon leached out of the biochars after rinsing the columns filled with sand and biochar with several litres of water prior to freeze–thaw cycling. We call this carbon fraction (after 240 mL of rinsing before any disintegration experiment) “baseline” and will refer to it as such in the following sections. This rinsing step was performed to ensure leached materials from the columns were mobilized because of cryostress and related experimental processes, rather than an artefact from column filling and/or biochar already disintegrated prior to the experiment (which would be mobilized in the first rinsing period).

3.1. Carbon loss from biochar subjected to physical stress and elution

Total carbon losses from biochar as quantified by TOC analyses of eluates were much higher in the shaking and sonication batch experiments than in the column experiments, indicating that simplified batch approaches may overestimate disintegration in the field (see Fig. 1). All experiments exhibited similar trends, though sonication was associated with larger standard deviations of replicates. Therein the particles >0.45 μm made up 58 ± 33 % of the total carbon mobilized, emphasizing that the micro- and nanosized mobilizable fraction is important for overall carbon losses from biochar.

Biochar disintegration and carbon loss was linked with the biochar's ash content (Table 1) as indicated by the higher stability of SWP550 and SWP700 compared to the remaining four biochars. This could be related to (macro)cavity formation caused by ash enclosure during biochar production and a subsequent solubilization of these encapsulated ash fractions (Spokas et al., 2014). Additionally, biochar disintegration increased with the degree of carbonization and aromaticity for both SWP and MSP based biochars. Chemical stability of biochar is typically

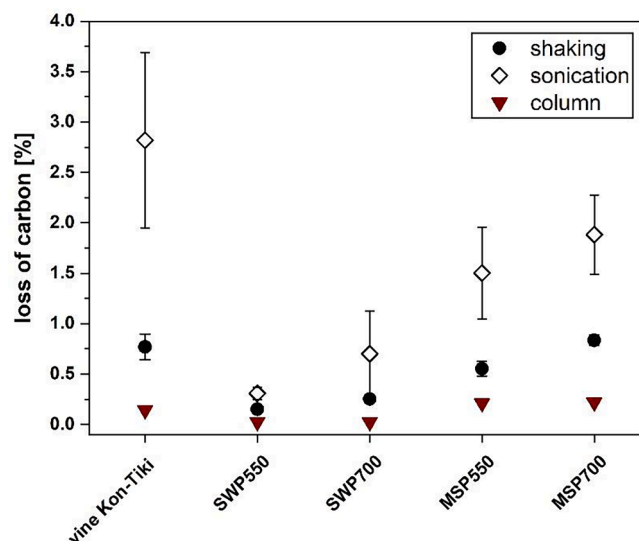


Fig. 1. Carbon loss in % mass from biochar at different experimental conditions quantified from TOC measurements of the eluate. With results from batch experiments in black, and column experiments in brown. The column data shown were measured at 120% water holding capacity after 80 freeze–thaw cycles, additional scenarios can be found in Fig. 2. Error bars represent standard deviation from three replicates.

Table 1

Bulk biochar properties including carbon content, molar H/C ratio, ash content, and total pore volume (TPV).

	Carbon [%]	H/C	Ash [%]	TPV [cm^3/g]
Kon-Tiki	75.72 ± 1.44	0.28 ± 0.03	9.32	0.095
SWP550	83.85 ± 2.20	0.35 ± 0.04	0.65	0.029
SWP700	84.73 ± 2.40	0.13 ± 0.03	0.99	0.119
MSP550	64.60 ± 2.79	0.38 ± 0.01	12.25	0.024
MSP700	79.18 ± 1.82	0.19 ± 0.02	10.09	0.029

associated with aromaticity (Wang et al., 2016). However, with increasing aromaticity and carbonization, the stiffness of the pyrolyzed biomass increases (Zickler et al., 2006), which could result in greater physical disintegration of these more brittle biochars, as indicated by our results.

3.2. Influence of freeze–thawing on carbon loss

After 80 freeze–thaw cycles, only approximately 0.2 % of carbon was mobilized from the biochars. The low biochar breakdown in our experiments can partially be explained by freezing point depression in small biochar pores. Most pores in the biochars were smaller than 2 nm as determined via N_2 physisorption. This pore size would decrease the freezing point of water by 8 to 12 °C following calculations by Wang et al., (2017). The freezing point is further decreased by ions in the artificial rain water and is more pronounced for unsaturated systems such as the 50 % WHC scenario (Zhou et al., 2018). Experimental results for Miscanthus based biochars after 80 freeze–thaw cycles are in line with a higher disintegration for 120 % WHC compared to 50 % WHC as shown in Fig. 2 (brown symbols). No such effect was observed for the other four biochars, presumably because they contained more micropores <2 nm and less mesopores (see Fig. S2).

In contrast, a larger proportion of carbon was mobilized from biochars in control columns that did not undergo freeze–thaw cycles (see Fig. 2). The increased carbon loss in the control columns compared to the frozen systems may partially be explained by a stronger wetting of internal pores and a slow dissolution processes which may have mobilized oxidized carbon fractions over the experimental duration (80

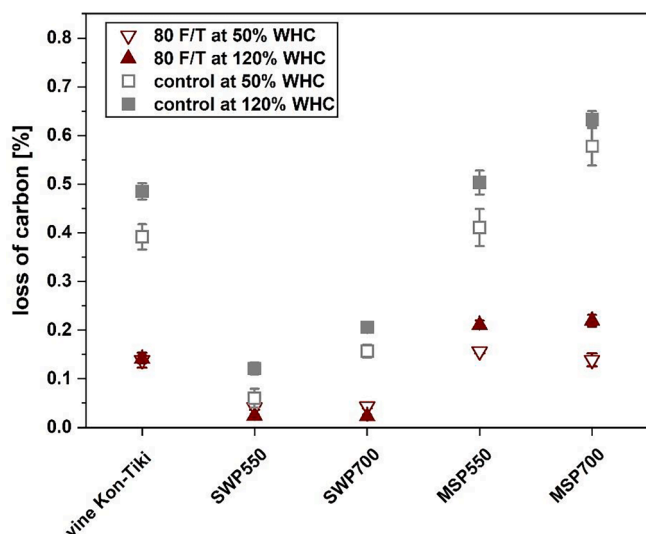


Fig. 2. Carbon loss in % mass from biochar-sand columns at different moisture levels with and without freeze-thaw cycling for 80 cycles quantified from TOC measurements of eluates. Error bars represent standard deviation from three replicates.

days). This hypothesis can partially be confirmed by an observed increase in carbon content by 10.70 ± 4.71 % throughout the different biochars (see Fig. S3) and a decrease in oxygen content by approximately 8.8 ± 6.8 % in the biochars recovered from the columns after the experiment. The higher mobilization of carbon from water saturated columns (120 % WHC) compared to the unsaturated columns (50 % WHC) is in good agreement with the hypothesis, that kinetically limited dissolution processes drove the mobilization of carbon in these experimental columns.

Our findings stand in some contrast with work by Liu et al. (2018) who found substantial physical biochar breakdown in the millimetre to centimetre range following 20 freeze-thaw cycles. However, the particle size range used in our experiments was smaller (0.25–1 mm) and Liu et al. did not quantify mobilized carbon in their experiments.

3.3. Characteristics of the mobilized carbon pool

The mobilized dissolved (<0.45 μm) organic matter leaching from biochar and other pyrogenic carbon materials is often referred to as “dissolved black carbon” (Qu et al., 2016; Xu et al., 2017; Wagner et al., 2021). Similarly to other researchers, we found that the least carbonized fraction was mobilized most easily from biochar, causing the carbon content in the residual bulk biochar to increase after experimentation. The specific ultraviolet absorbance at 254 nm normalized to DOC (SUVA_{254}) is linked to the aromaticity of the dissolved organic carbon (Weishaar et al., 2003). When comparing measured SUVA_{254} between DOC fractions from pre-rinsing (“baseline”) and after 80 freeze-thaw cycles, over time more aromatic fractions were mobilized, as shown in Fig. 3 (SUVA_{254} increased for all biochars except for the Kon-Tiki sample). This is in good agreement with findings by Abiven et al. (2011) who found that the carbon fraction leached from aged wildfire charcoal was more aromatic compared to fresh charcoals produced from the same feedstock (chestnut wood).

In addition to the increasingly aromatic dissolved carbon fractions (<0.45 μm), carbonaceous micro- and nanoparticles were also mobilized during experiments. The overwhelming majority of particles mobilized in column experiments were <10 μm with number based median grain sizes ranging from 1 to 4 μm (see Fig. 4 and Fig. S4). Due to the higher physical stress in the shaking experiments, larger fractions of the biochar broke of, resulting in larger median grain sizes in these samples compared to particles mobilized in the column experiments. In contrast,

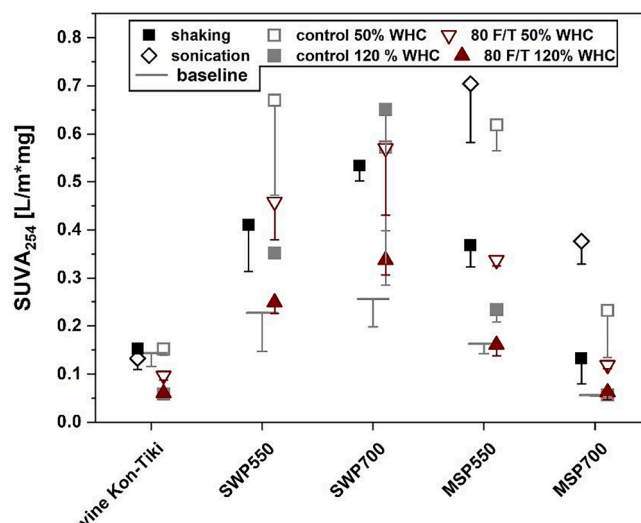


Fig. 3. Specific ultraviolet absorbance at 254 nm (SUVA_{254}) for DOC fractions leached from biochars in shaking and sonication batch experiments, columns before freeze-thaw cycles (baseline), columns after 80 days without freeze-thaw cycling (control) at different water holding capacities (WHC) and columns after 80 freeze-thaw cycles (80 F/T). Error bars are shown only downwards to increase readability and represent standard deviation from three replicates.

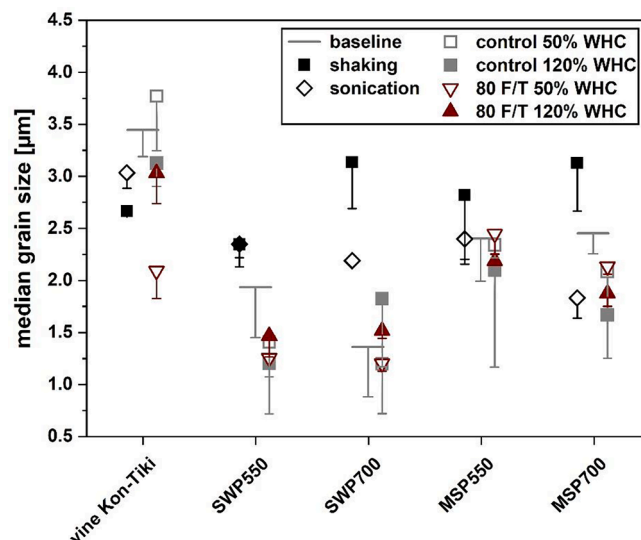


Fig. 4. Median Grain Size (D50) of number-based particle size distributions for carbonaceous particles mobilized from the bulk biochars in shaking and sonication batch experiments, columns before freeze-thaw cycles (baseline), columns after 80 days without freeze-thaw cycling (control) at different water holding capacities (WHC), and columns after 80 freeze-thaw cycles (80 F/T). Error bars are shown only downwards to increase readability and represent standard deviations from three replicates.

sonication did not result in larger particle sizes, presumably because the physical stress from the sonication further broke down any larger biochar particle that may detached from the bulk material, as indicated by the largest carbon fraction being mobilized with sonication for all biochars (Fig. 1).

All biochars investigated released negatively charged particles, as indicated by the measured negative zeta potential ranging from -10 to -30 mV (Fig. S5). Such zeta potentials can be associated to electrostatic stabilisation and supporting mobility in negatively charged sand systems as investigated here (Peijnenburg et al., 2015; Sigmund et al., 2018). In

the presence of clay these particles can form biochar-clay aggregates via electrostatic interactions with positively charged edges of clay minerals, organometallic complexes with iron containing minerals and/or via physical entrapment (Yang et al., 2016). The carbon encapsulated in such mineral associated forms is expected to be among the most stable carbon pools in soil (Gui et al., 2021; Yang et al., 2022). An increase in biochar carbon stability in clay containing soils is well documented and confirms this phenomenon (Wang et al., 2016; Yang et al., 2022). However, in very sandy systems at moderate to high pH as investigated here, small particles could still be mobilized and subsequently degraded microbially in soils and/or photochemically in surface waters (Bird et al., 2015).

4. Conclusions

The physical disintegration of biochar has previously been postulated to be a determining factor for biochar persistence. In this study, we focused on small biochar particles (0.25–1 mm) and their potential disintegration, measuring carbon contents of the fractions released, including carbonaceous micro- and nanoparticles. These particles did not strongly disintegrate after freeze–thaw cycling, possibly because of freezing point depression in the very small pores in the biochar. When comparing different biochars we found that those with larger ash fractions were less stable, presumably because of ash-associated formation of unstable cavities within the biochar. Further, we observed a decreased physical stability of biochars with increasing aromaticity (when comparing biochars from the same feedstock at different pyrolysis temperatures), which could be linked to a higher rigidity of more aromatic structures. Our results further suggest that moisture content in the soil is a more important factor for the mobilization of carbon from biochar compared to physical stress such as freeze–thaw cycling.

While physical disintegration of biochar should not be neglected as a source of more labile carbon from bulk biochar, and the nano- and micronized particles can be mobilized in the subsurface under certain conditions (limited or no clay, moderate to high pH), in most soils these carbon fractions will be in contact with clay at some point in time, which would strongly reduce their mobility. The physical disintegration of biochar and subsequent mobilization of micro- and nanosized carbon should thus be considered of minor relevance and is often not a driving factor for biochar stability compared to chemical oxidation and biological degradation of the bulk biochar.

CRedit authorship contribution statement

Gabriel Sigmund: Conceptualization, Supervision, Data curation, Formal analysis, Writing – original draft, Visualization. **Andrea Schmid:** Methodology, Data curation, Formal analysis. **Hans-Peter Schmidt:** Conceptualization, Writing – review & editing. **Nikolas Hagemann:** Conceptualization, Writing – review & editing. **Thomas D. Bucheli:** Conceptualization, Writing – review & editing. **Thilo Hofmann:** Writing – review & editing.

Declaration of Competing Interest

The authors declare that they have no known competing financial interests or personal relationships that could have appeared to influence the work reported in this paper.

Data availability

The data used in this study have been deposited in the Zenodo public data repository at <https://doi.org/10.5281/zenodo.6556349>.

Appendix A. Supplementary data

Supplementary data to this article can be found online at <https://doi.org/10.1016/j.geoderma.2023.116326>.

[org/10.1016/j.geoderma.2023.116326](https://doi.org/10.1016/j.geoderma.2023.116326).

References

- Abiven, S., Hengartner, P., Schneider, M.P.W., Singh, N., Schmidt, M.W.I., 2011. Pyrogenic carbon soluble fraction is larger and more aromatic in aged charcoal than in fresh charcoal. *Soil Biol. Biochem.* 43, 1615–1617. <https://doi.org/10.1016/j.soilbio.2011.03.027>.
- Bird, M.I., Wynn, J.G., Saiz, G., Wurster, C.M., McBeath, A., 2015. The pyrogenic carbon cycle. *Annu. Rev. Earth Planet. Sci.* 43, 273–298. <https://doi.org/10.1146/annurev-earth-060614-105038>.
- Bowring, S.P.K., Jones, M.W., Ciaia, P., Guenet, B., Abiven, S., 2022. Pyrogenic carbon decomposition critical to resolving fire's role in the Earth system. *Nat. Geosci.* 15, 135–142. <https://doi.org/10.1038/s41561-021-00892-0>.
- Brewer, C.E., Chuang, V.J., Masiello, C.A., Gonnermann, H., Gao, X., Dugan, B., Driver, L. E., Panzacchi, P., Zygourakis, K., Davies, C.A., 2014. New approaches to measuring biochar density and porosity. *Biomass Bioenergy* 66, 176–185. <https://doi.org/10.1016/j.biombioe.2014.03.059>.
- Freeze-Thaw Days: https://www.atlas.impact2c.eu/en/climate/freeze-thaw-days/?parent_id=22, last access: 25 April 2022.
- Edeh, I.G., Masek, O., Buss, W., 2020. A meta-analysis on biochar's effects on soil water properties – New insights and future research challenges. *Sci. Total Environ.* 714, 136857 <https://doi.org/10.1016/j.scitotenv.2020.136857>.
- Gui, X., Song, B., Chen, M., Xu, X., Ren, Z., Li, X., Cao, X., 2021. Soil colloids affect the aggregation and stability of biochar colloids. *Sci. Total Environ.* 771, 145414 <https://doi.org/10.1016/j.scitotenv.2021.145414>.
- Keilueit, M., Nico, P.S., Johnson, M.G., Kleber, M., 2010. Dynamic molecular structure of plant biomass-derived black carbon (biochar). *Environ. Sci. Technol.* 44, 1247–1253. <https://doi.org/10.1021/es9031419>.
- Liu, Z., Dugan, B., Masiello, C.A., Wahab, L.M., Gonnermann, H.M., Nitttrouer, J.A., Paz-Ferreiro, J., 2018. Effect of freeze-thaw cycling on grain size of biochar. *PLoS One* 13 (1), e0191246.
- Peijnenburg, W.J.G.M., Baalousha, M., Chen, J., Chaudry, Q., Von Der Kammer, F., Kuhlbusch, T.A.J., Lead, J., Nickel, C., Quik, J.T.K., Renker, M., Wang, Z., Koelmans, A.A., 2015. A review of the properties and processes determining the fate of engineered nanomaterials in the aquatic environment. *Crit. Rev. Environ. Sci. Technol.* 45, 2084–2134. <https://doi.org/10.1080/10643389.2015.1010430>.
- Qu, X., Fu, H., Mao, J., Ran, Y., Zhang, D., Zhu, D., 2016. Chemical and structural properties of dissolved black carbon released from biochars. *Carbon* 96, 759–767. <https://doi.org/10.1016/j.carbon.2015.09.106>.
- Ricci, M., de Vos, E., Oostru, A., 2010. Certification of the mass concentrations of ammonium, chloride, fluoride, magnesium, nitrate, ortho-phosphate, sulfate, and of pH and conductivity in simulated rainwater: certified reference material ERM-CA408. Publications Office, LU.
- Santin, C., Doerr, S.H., Merino, A., Bucheli, T.D., Bryant, R., Ascough, P., Gao, X., Masiello, C.A., 2017. Carbon sequestration potential and physicochemical properties differ between wildfire charcoals and slow-pyrolysis biochars. *Sci. Rep.* 7, 1–11. <https://doi.org/10.1038/s41598-017-10455-2>.
- Schiedung, M., Belle, S.-L., Sigmund, G., Kalbitz, K., Abiven, S., 2020. Vertical mobility of pyrogenic organic matter in soils: a column experiment. *Biogeosciences* 17, 6457–6474. <https://doi.org/10.5194/bg-17-6457-2020>.
- Sigmund, G., Hüffer, T., Hofmann, T., Kah, M., 2017. Biochar total surface area and total pore volume determined by N₂ and CO₂ physisorption are strongly influenced by degassing temperature. *Sci. Total Environ.* 580, 770–775. <https://doi.org/10.1016/j.scitotenv.2016.12.023>.
- Sigmund, G., Jiang, C., Hofmann, T., Chen, W., 2018. Environmental transformation of natural and engineered carbon nanoparticles and implications for the fate of organic contaminants. *Environ. Sci. Nano* 5 (11), 2500–2518.
- Song, B., Chen, M., Zhao, L., Qiu, H., Cao, X., 2019. Physicochemical property and colloidal stability of micron- and nano-particle biochar derived from a variety of feedstock sources. *Sci. Total Environ.* 661, 685–695. <https://doi.org/10.1016/j.scitotenv.2019.01.193>.
- Spokas, K.A., Novak, J.M., Masiello, C.A., Johnson, M.G., Colosky, E.C., Ippolito, J.A., Trigo, C., 2014. Physical disintegration of biochar: an overlooked process. *Environ. Sci. Technol. Lett.* 1, 326–332. <https://doi.org/10.1021/ez500199t>.
- Wagner, S., Coppola, A.L., Stubbins, A., Dittmar, T., Niggemann, J., Drake, T.W., Seidel, M., Spencer, R.G.M., Bao, H., 2021. Questions remain about the biolability of dissolved black carbon along the combustion continuum. *Nat. Commun.* 12, 4281. <https://doi.org/10.1038/s41467-021-24477-y>.
- Wang, C., Lai, Y., Zhang, M., 2017. Estimating soil freezing characteristic curve based on pore-size distribution. *Appl. Therm. Eng.* 124, 1049–1060. <https://doi.org/10.1016/j.applthermaleng.2017.06.006>.
- Wang, J., Xiong, Z., Kuzyakov, Y., 2016. Biochar stability in soil: Meta-analysis of decomposition and priming effects. *GCB Bioenergy* 8, 512–523. <https://doi.org/10.1111/gcbb.12266>.
- Weishaar, J.L., Aiken, G.R., Bergamaschi, B.A., Fram, M.S., Fujii, R., Mopper, K., 2003. Evaluation of specific ultraviolet absorbance as an indicator of the chemical composition and reactivity of dissolved organic carbon. *Environ. Sci. Technol.* 37, 4702–4708. <https://doi.org/10.1021/es030360x>.
- Xing, B., Liu, G., Zheng, H., Jiang, Z., Zhao, J., Wang, Z., Pan, B., Xing, B., 2018. Formation and physicochemical characteristics of nano biochar: insight into chemical and colloidal stability. *Environ. Sci. Technol.* 52 <https://doi.org/10.1021/acs.est.8b01481>.
- Xu, F., Wei, C., Zeng, Q., Li, X., Alvarez, P.J.J., Li, Q., Qu, X., Zhu, D., 2017. Aggregation behavior of dissolved black carbon: implications for vertical mass flux and

- fractionation in aquatic systems. *Environ. Sci. Technol.* 51, 13723–13732. <https://doi.org/10.1021/acs.est.7b04232>.
- Yang, Y., Sun, K., Han, L., Chen, Y., Liu, J., Xing, B., 2022. Biochar stability and impact on soil organic carbon mineralization depend on biochar processing, aging and soil clay content. *Soil Biol. Biochem.* 169, 108657 <https://doi.org/10.1016/j.soilbio.2022.108657>.
- Yang, F., Zhao, L., Gao, B., Xu, X., Cao, X., 2016. The interfacial behavior between biochar and soil minerals and its effect on biochar stability. *Environ. Sci. Technol.* 50, 2264–2271. <https://doi.org/10.1021/acs.est.5b03656>.
- Zhou, J., Wei, C., Lai, Y., Wei, H., Tian, H., 2018. Application of the generalized clapeyron equation to freezing point depression and unfrozen water content. *Water Resour. Res.* 54, 9412–9431. <https://doi.org/10.1029/2018WR023221>.
- Zickler, G.A., Schöberl, T., Paris, O., 2006. Mechanical properties of pyrolysed wood: a nanoindentation study, 86, 1373–1386. *Phil. Mag.* 86 (10), 1373–1386.